IMU and Passive Resonator Localization System for Autonomous Vehicles

Isaac Froisland

Electrical and Computer Engineering Department,
Utah State University
Logan, UT 84321
isaac.froisland@gmail.com

I. INTRODUCTION

All-electric autonomous vehicles (AVs) carry many advantages over internal-combustion and non-autonomous modes of transportation. Existing obstacles to widespread adoption of electric AVs include limited battery energy storage, initial cost, and the current limitations of vehicle automation. One approach to addressing these issues is the development of "connected autonomous vehicles" (CAVs) [4]. CAVs can rely on communication with a network of other connected vehicles and information systems to determine the state of the vehicle and its surroundings. CAVs can also benefit from dynamic wireless power transfer (DWPT), sometimes called "in-lane charging." DWPT for electric vehicles uses a primary coil embedded in the roadway to transmit power to a secondary coil on the vehicle. DWPT mitigates the initial cost and limited battery energy storage of electric AVs by decreasing required battery capacity and providing opportunities to recharge without stopping the vehicle. DWPT relies on precise alignment between the coils (on a scale of centimeters), and this precise alignment requires accurate state measurements of the vehicle. Current AV technology has difficulty determining vehicle state in rain, snow, and other poor visibility conditions due to its reliance on visual line-of-sight sensors and imprecise or limited GPS. Current localization technology also suffers from high power requirements and expensive computational hardware.

A. Literature Review

Existing research on vehicle localization has considered systems that do not use line-of-sight sensors (LiDAR and cameras) or GPS. Cortes [1] developed a method to sense lateral misalignment in inductive power transmission wireless charging systems using received signal strength indicator (RSSI) measurements. Cortes's research focused on static charging systems, determining the impact of vertical and horizontal spacing of the primary and secondary coils on position measurements. The results show that misalignment direction can be determined consistently with RSSI measurements, but misalignment magnitude is difficult to determine from the non-linear signal output of the sensing coils.

In [6], a phase difference of arrival (PDOA) method is used with RFID tags to localize mobile robots in an indoor environment. Compared to using a RSSI method, the PDOA method proved through simulation to have less error. The PDOA method is less susceptible to multipath signal propagation. The researchers in [6] also implemented a Kalman Filter to fuse relative positioning data from encoders with the absolute positioning data from the RFID tags. In a similar study, Hekimian-Williams et al [3] conducted physical experiments that showed localization accuracy on a scale of millimeters is achievable with a RFID PDOA system. Hekimian-Williams et al indicated how physical experiment results are directly relevant to localization applications (as opposed to purely simulated results), but it should be taken into account that the physical experiment results may depend on ideal conditions.

Other work has focused on localization in GPS-denied or GPS-limited environments. Whitaker et al [5] conducted simulations to determine the performance of "self-describing fiducials" fused with IMU data via an extended Kalman Filter (EKF) for ground-vehicle localization in GPS-denied environments. Similar fiducials are commonly used with cell-phone cameras to give the phone information relevant to the marker location. Whitaker et al determined that such a system is heavily dependent on sensor quality, but the system could provide acceptable error levels even with a consumer grade IMU. Future work along this track could include incorporating fiducial location uncertainty into the model.

Costley and Christensen in [2] developed a navigation framework that incorporates LiDAR object detection with IMU measurements to work in GPS-limited environments. The LiDAR object detection and IMU measurements are fused via an EKF to estimate the state of simulated vehicle in an orchard. The paper provides a performance evaluation that compares the position estimate error covariance of the system with the LiDAR measurements and without LiDAR. The results show a minimum of 90% improvement in 3-σ deviation for the system incorporating LiDAR over the system that did not incorporate LiDAR.

B. Proposed Contribution

This work proposes a simulation to predict the performance of a localization system for road vehicles utilizing an industrial grade IMU and PDOA method using passive circuit resonators. The PDOA method will be similar to the technology used in [6] and [3]. IMU data will be used to propagate the state of the vehicle and PDOA data will be

used for state updates. Data from both subsystems will be fused via an EKF to estimate vehicle state. Performance will be measured by position estimate error covariance, and the system incorporating PDOA measurements will be compared to a system that uses an IMU and GPS. The sensitivity of the design to measurement errors, road coil spacing, and vehicle coil configuration will be analyzed. After determining the performance of the proposed system, the feasibility of using such a system for DWPT alignment and general vehicle automation will be considered.

II. STATE VECTORS

A. Coordinate System

The coordinate system, truth state, design state, navigation state, and error state will be defined in this section. Mappings between states to be used in the simulation will be determined and verified via a numerical example.

To predict the performance of the localization system, a Monte Carlo simulation will be used. The simulated vehicle will have dimensions similar to a common road vehicle. To simplify the problem, it is assumed that the IMU is mounted rigidly in relation to the PDOA system. This means that the position and orientation of the IMU relative to the PDOA system can be measured with negligible uncertainty. Figure 1 shows the coordinate system and vectors that will be used to define the state vectors. The
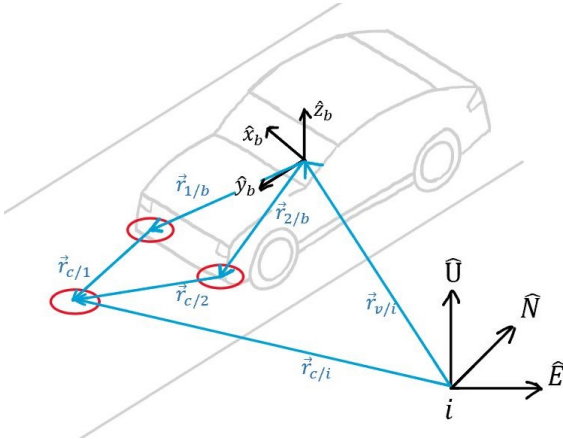

Fig. 1. Coordinate System of IMU and PDOA System

vectors in the coordinate system are described as follows:

$\hat{N}, \hat{E}, \hat{U}$ = North, East, and Up unit vectors of inertial frame.
$\hat{x}_b, \hat{y}_b, \hat{z}_b$ = Unit vectors of the body frame.
$\vec{r}_{v/i}$ = Vehicle position in inertial frame.
$\vec{r}_{1/b}$ = Sensing coil 1 position in body frame.
$\vec{r}_{2/b}$ = Sensing coil 2 position in body frame.
$\vec{r}_{c/1}$ = Ground coil position in sensing coil 1 frame.
$\vec{r}_{c/2}$ = Ground coil position in sensing coil 2 frame.
$\vec{r}_{c/i}$ = Ground coil position in inertial frame.

B. State Vector Definitions

Truth State: the actual state of the system.
Design State: includes the components of the truth state that need to be estimated by the Kalman filter.

Navigation State: the estimated state of the system with components corresponding to those of the design state.
Error State: defines the error between the design state and navigation state.

The truth state vector is $\vec{x}_t$:

$$\vec{x}_t = \begin{bmatrix} \vec{r}_v & \vec{v}_v & q_v & \vec{\omega}_v & \phi & \vec{b}_a & \vec{b}_g & \vec{r}_c \end{bmatrix}^T \quad (1)$$

The components of $\vec{x}_t$ are: (component dimension in braces)

$\vec{r}_v$ = vehicle position {3},
$\vec{v}_v$ = vehicle velocity {3},
q_v = vehicle attitude {4},
$\vec{\omega}_v$ = vehicle angular rate {3},
ϕ = vehicle steering angle {1},
$\vec{b}_a$ = accelerometer bias {3},
$\vec{b}_g$ = gyroscope bias {3},
$\vec{r}_c$ = ground circuit position {3},

where $\vec{r}_v$, $\vec{v}_v$, q_v, $\vec{\omega}_v$, and $\vec{r}_c$ are measured in the inertial frame. q_v is an attitude quaternion.

$\vec{\omega}_v$ is measured directly from the gyroscope, and ϕ is a function of $\vec{\omega}_v$. Because $\vec{\omega}_v$ and ϕ do not have to be estimated, the design state vector ($\vec{x}$) can omit them. $\vec{x}_t$ can be mapped to $\vec{x}$ with a matrix multiplication. The subscripts of the identity matrices indicate dimension:

$$\vec{x} = \vec{m}(\vec{x}_t) = \begin{bmatrix} I_3 & 0 & 0 & 0 & 0 & 0 & 0 \\ 0 & I_3 & 0 & 0 & 0 & 0 & 0 \\ 0 & 0 & I_4 & 0 & 0 & 0 & 0 \\ 0 & 0 & 0 & 0 & I & 0 & 0 \\ 0 & 0 & 0 & 0 & 0 & I & 0 \\ 0 & 0 & 0 & 0 & 0 & 0 & I \end{bmatrix} \begin{bmatrix} \vec{r}_v \\ \vec{v}_v \\ q_v \\ \vec{\omega}_v \\ \phi \\ \vec{b}_a \\ \vec{b}_g \\ \vec{r}_c \end{bmatrix} \quad (2)$$

$$\vec{x} = \begin{bmatrix} \vec{r}_v & \vec{v}_v & q_v & \vec{b}_a & \vec{b}_g & \vec{r}_c \end{bmatrix}^T \quad (3)$$

The navigation state vector $\hat{x}$ has estimated components corresponding to those of $\vec{x}$:

$$\hat{x} = \begin{bmatrix} \hat{r}_v & \hat{v}_v & \hat{q}_v & \hat{b}_a & \hat{b}_g & \hat{r}_c \end{bmatrix}^T \quad (4)$$

The error state vector is $\vec{\delta x}$:

$$\vec{\delta x} = \begin{bmatrix} \vec{\delta r}_v & \vec{\delta v}_v & \vec{\delta \theta}_v & \vec{\delta b}_a & \vec{\delta b}_g & \vec{\delta r}_c \end{bmatrix}^T \quad (5)$$

where each component has a dimension of {3}. In $\vec{\delta x}$, $\vec{\delta \theta}_v$ is a vector that has a dimension of {3} that replaces the q_v and $\hat{q}_v$ with dimensions of {4} found in $\vec{x}_t$ and $\vec{x}$, respectively. This is because only the vector component of the quaternion needs to be estimated. The scalar component will always be approximately equal to 1. That is (using a small angle approximation of $sin\,\theta \approx \theta$ and $cos\,\theta \approx 1$),

$$q_v = \begin{bmatrix} cos(\theta/2) \\ \vec{k} sin(\theta/2) \end{bmatrix} \approx \begin{bmatrix} 1 \\ \vec{\theta}/2 \end{bmatrix}$$

C. State Vector Mappings

$\vec{x}$ can be related to $\hat{x}$ and $\vec{\delta x}$ by defining the following error correction mapping:

$$\vec{x} = \vec{c}(\hat{x}, \vec{\delta x}) = \begin{bmatrix} \vec{r}_v \\ \vec{v}_v \\ q_v \\ \vec{b}_a \\ \vec{b}_g \\ \vec{r}_c \end{bmatrix} = \begin{bmatrix} \hat{r}_v + \vec{\delta r}_v \\ \hat{v}_v + \vec{\delta v}_v \\ \begin{bmatrix} 1 \\ \vec{\delta\theta}_v/2 \end{bmatrix} \otimes \hat{q}_v \\ \hat{b}_v + \vec{\delta b}_a \\ \hat{b}_a + \vec{\delta b}_g \\ \hat{r}_c + \vec{\delta r}_c \end{bmatrix} \quad (6)$$

where $\otimes$ denotes quaternion multiplication.

(6) can be manipulated to produce an error injection mapping:

$$\hat{x} = \vec{i}(\vec{x}, \vec{\delta x}) = \begin{bmatrix} \hat{r}_v \\ \hat{v}_v \\ \hat{q}_v \\ \hat{b}_v \\ \hat{b}_a \\ \hat{r}_c \end{bmatrix} = \begin{bmatrix} \vec{r}_v - \vec{\delta r}_v \\ \vec{v}_v - \vec{\delta v}_v \\ \begin{bmatrix} 1 \\ -\vec{\delta\theta}_v/2 \end{bmatrix} \otimes q_v \\ \vec{b}_a - \vec{\delta b}_a \\ \vec{b}_g - \vec{\delta b}_g \\ \vec{r}_c - \vec{\delta r}_c \end{bmatrix} \quad (7)$$

(7) will be used to inject errors into the state estimation vector $\hat{x}$ in the simulation. Those errors are computed using an estimation error mapping, which can be found by manipulating (7):

$$\vec{\delta x} = \vec{e}(\vec{x}, \hat{x}) = \begin{bmatrix} \vec{\delta r}_v \\ \vec{\delta v}_v \\ \vec{\delta\theta}_v \\ \vec{\delta b}_a \\ \vec{\delta b}_g \\ \vec{\delta r}_c \end{bmatrix} = \begin{bmatrix} \vec{r}_v - \hat{r}_v \\ \vec{v}_v - \hat{v}_v \\ f(\vec{\delta q}) \\ \vec{b}_v - \hat{b}_v \\ \vec{b}_a - \hat{b}_a \\ \vec{r}_c - \hat{r}_c \end{bmatrix} \quad (8)$$

where $\vec{\delta q} = q_v \otimes (\hat{q}_v)^*$ and $f(\vec{\delta q})$ is the last 3 elements of $\vec{\delta q}$ multiplied by 2.

D. Mapping Verification

The following initial conditions ($\vec{x}_0$) and injected errors ($\vec{\delta x}_i$) are used to verify consistency between mappings (2), (6), (7), and (8):

The mapping verification process will be as follows:

1) Mapping (2) will be used to map the initial conditions to the design state vector (3).
2) Mapping (7) will be used to inject errors into the design state vector to produce the navigation state vector (4).
3) Mapping (8) will be used to calculate the errors in the navigation state vector to produce the error state vector (5).
4) Mapping (6) will finally be used to correct the errors in the navigation state vector to reproduce the design state vector (3).

MATLAB code is used to perform all of the calculations. Within the MATLAB code, the injected errors (shown in Table I) will be compared to the errors calculated in step 3. The navigation state vector produced in step 2 will also be compared with the design state vector produced

TABLE I
INITIAL CONDITIONS OF $\vec{x}$ AND VALUES OF INJECTED $\vec{\delta x}$ USED TO VERIFY MAPPINGS BETWEEN STATE VECTORS

$\vec{x}$	$\vec{x}_0$	Units	$\vec{\delta x}$	$\vec{\delta x}_i$	Units
$\vec{r}_v$	$\begin{bmatrix} 0 \\ 0 \\ 0.15 \end{bmatrix}$	$[m]$	$\vec{\delta r}_v$	$\begin{bmatrix} 0.1 \\ 0.2 \\ 0.3 \end{bmatrix}$	$[m]$
$\vec{v}_v$	$\begin{bmatrix} 0.25 \\ 1 \\ 0 \end{bmatrix}$	$[\frac{m}{s}]$	$\vec{\delta v}_v$	$\begin{bmatrix} 1 \\ 2 \\ 3 \end{bmatrix}$	$[\frac{m}{s}]$
q	$\begin{bmatrix} 1 \\ 0 \\ 0 \\ 0 \end{bmatrix}$	[unitless]	$\vec{\delta\theta}_v$	$\begin{bmatrix} 0.01 \\ 0.02 \\ 0.03 \end{bmatrix}$	$[rad]$
$\vec{b}_a$	$\begin{bmatrix} 0 \\ 0 \\ 0 \end{bmatrix}$	$[g]$	$\vec{\delta b}_a$	$\begin{bmatrix} 0.001 \\ 0.002 \\ 0.003 \end{bmatrix}$	$[g]$
$\vec{b}_g$	$\begin{bmatrix} 0 \\ 0 \\ 0 \end{bmatrix}$	$[\frac{deg}{hr}]$	$\vec{\delta b}_g$	$\begin{bmatrix} 1 \\ 2 \\ 3 \end{bmatrix}$	$[\frac{deg}{hr}]$
$\vec{r}_c$	$\begin{bmatrix} 0 \\ 1 \\ 0 \end{bmatrix}$	$[m]$	$\vec{\delta r}_c$	$\begin{bmatrix} 0.11 \\ 0.22 \\ 0.33 \end{bmatrix}$	$[m]$

in step 4. Verification steps in the code will confirm that corresponding vectors have differences of less than $1e^{-10}$.

Table II compares the design state vector produced in step 1 ($\vec{x}_1$) to the design state vector produced in step 4 ($\vec{x}_4$). The table shows high computational fidelity through the sequence of state vector mappings.

TABLE II
DESIGN STATE VECTOR COMPARED ACROSS MAPPING SEQUENCE

$\vec{x}_1$	$\vec{x}_4$	Difference
0.000000000000000	0.000000000000000	0.000000000000000
0.000000000000000	0.000000000000000	0.000000000000000
0.150000000000000	0.150000000000000	0.000000000000000
0.250000000000000	0.250000000000000	0.000000000000000
1.000000000000000	1.000000000000000	0.000000000000000
0.000000000000000	0.000000000000000	0.000000000000000
1.000000000000000	1.000000000000000	0.000000000000000
0.000000000000000	0.000000000000000	0.000000000000000
0.000000000000000	0.000000000000000	0.000000000000000
0.000000000000000	0.000000000000000	0.000000000000000
0.000000000000000	0.000000000000000	0.000000000000000
0.000000000000000	0.000000000000000	0.000000000000000
0.000000000000000	0.000000000000000	0.000000000000000
0.000000000000000	0.000000000000000	0.000000000000000
0.000000000000000	0.000000000000000	0.000000000000000
0.000000000000000	0.000000000000000	0.000000000000000
0.000000000000000	0.000000000000000	0.000000000000000
1.000000000000000	1.000000000000000	0.000000000000000
0.000000000000000	0.000000000000000	0.000000000000000

REFERENCES

[1] Ivan Cortes. "Automatic Positioning System for Inductive Wireless Charging Devices and Application to Mobile Robot". en. Accepted: 2018-02-05T21:16:43Z. Thesis. July 2017. URL: https://oaktrust.library.tamu.edu/handle/1969.1/165925 (visited on 09/20/2021).

[2] Austin Costley and Randall Christensen. "Landmark Aided GPS-Denied Navigation for Orchards and Vineyards". In: *2020 IEEE/ION Position, Location and Navigation Symposium (PLANS)*. ISSN: 2153-3598. Apr. 2020, pp. 987–995. DOI: 10.1109/PLANS46316.2020.9110130.

[3] Cory Hekimian-Williams et al. "Accurate localization of RFID tags using phase difference". In: *2010 IEEE International Conference on RFID (IEEE RFID 2010)*. ISSN: 2374-0221. Apr. 2010, pp. 89–96. DOI: 10.1109/RFID.2010.5467268.

[4] Margarita Martínez-Díaz and Francesc Soriguera. "Autonomous vehicles: theoretical and practical challenges". en. In: *Transportation Research Procedia*. XIII Conference on Transport Engineering, CIT2018 33 (Jan. 2018), pp. 275–282. ISSN: 2352-1465. DOI: 10.1016/j.trpro.2018.10.103. URL: https://www.sciencedirect.com/science/article/pii/S2352146518302606 (visited on 09/21/2021).

[5] Justin Whitaker, Randall Christensen, and Greg Droge. "Global Localization of Ground Vehicles Using Self-Describing Fiducials Coupled with IMU Data". In: *2020 IEEE/ION Position, Location and Navigation Symposium (PLANS)*. ISSN: 2153-3598. Apr. 2020, pp. 186–196. DOI: 10.1109/PLANS46316.2020.9109829.

[6] Yunlei Zhang et al. "Localization and Tracking of an Indoor Autonomous Vehicle Based on the Phase Difference of Passive UHF RFID Signals". en. In: *Sensors* 21.9 (May 2021), p. 3286. ISSN: 1424-8220. DOI: 10.3390/s21093286. URL: https://www.mdpi.com/1424-8220/21/9/3286 (visited on 09/20/2021).